Asian Journal of Chemistry; Vol. 23, No. 6 (2011), 2696-2700

ASIAN JOURNAL OF CHEMISTRY

www.asianjournalofchemistry.co.in

Thermoluminescence Studies on Li_2O-MO-B_2O_3 Glasses Doped with Rare Earth Ions

J. ANJAIAH[1,*], C. LAXMI KANTH[2], Y. RANGA REDDY[3] and P. KISTAIAH[4]

[1]Department of Physics, Geethanjali College of Engineering and Technology, Keesara, RR Dist.-501 301, India
[2]Department of Physics, Eritrea Institute of Technology, Asmara, Eritrea (North-East Africa)
[3]Vidya Bharathi Institute of Technology, Pembarthi, Jangaon, Warangal-506 201, India
[4]Department of Physics, University College of Science, Osmania University, Hyderabad-500 007, India

*Corresponding author: E-mail: anjaiah.juluru@gmail.com

(*Received*: 5 September 2010; *Accepted*: 18 February 2011) AJC-9642

Thermoluminescence (TL) characteristics of X-ray irradiated pure and doped with four different rare earth ions (*viz*., Pr^{3+}, Nd^{3+}, Sm^{3+} and Eu^{3+}) lithium borate glasses mixed with the three different modifiers ZnO, CaO and CdO have been studied in 303-573 K. All the pure glasses have exhibited single thermoluminescence peak at 382, 424 and 466 K, respectively. When these glasses are doped with different rare earth ions no additional peaks are observed but the glow peak temperature of the existing glow peak shifted gradually towards higher temperatures with gain in intensity of thermoluminescence light output. The area under the glow curve is also found to be maximum for Eu^{3+} doped glasses. The glasses containing CdO as modifier have exhibited the maximum thermoluminescence light output. The trap depth parameters associated with the observed thermoluminescence peaks have been evaluated using Chen's formulae. The possible use of these glasses in radiation dosimetry has been described.

Key Words: Thermoluminesence, Lithium borate glasses, Glass modifiers, Radiation dosimetry.

INTRODUCTION

The understanding of the glass structure by detailed studies on radiation induced defect centres has been an interesting subject of investigation in recent years. Pontuschka *et al.*[1-4] have done a recommendable work on thermoluminescence mechanisms in borate glasses. Borate glasses are very advantageous materials for the radiation dosimetry applications in view of the fact that their effective atomic number is very close to that of human tissue. However, pure borate glasses have certain disadvantages to use in radiation dosimetry since they are highly hygroscopic and exhibit weak glow peak at relatively low temperatures. Alkali oxy borate glasses are considered as good materials for dosimetry applications since they are relatively moisture resistant when compared with the pure borate glasses.

The study on the influence of rare earth ions on thermoluminescence light output of these glasses is also carried out with a view to examine the suitability of these glasses in the radiation dosimetry.

EXPERIMENTAL

For the present study the following compositions in mol % are chosen: **ZnBLn series:** 30Li_2O-10ZnO - (60-x) B_2O_3: 1Ln_2O_3, **CaBLn series:** 30Li_2O-10CaO - (60-x) B_2O_3: 1Ln_2O_3 and **CdBLn series:** 30Li_2O - 10CdO - (60-x) B_2O_3: 1Ln_2O_3; (where x = 0 and 1 and Ln^{3+} = Pr^{3+}, Nd^{3+}, Sm^{3+} and Eu^{3+}).

The glasses used for the present study are prepared by the melting and quenching techniques[5-7]. The starting materials used for the preparation of the present glasses were analytical grade reagents (99.9 % pure) of CdO, $CaCO_3$, ZnO, H_3BO_3, Li_2CO_3, Pr_2O_3, Nd_2O_3, Sm_2O_3 and Eu_2O_3. These materials in mole % were thoroughly mixed in an agate mortar and melted in a platinum crucible. These compositions were heated and maintained at 450 ºC for 2 h for the decarbonisation from $CaCO_3$ and Li_2CO_3 and then the temperature was raised up to 1050 ºC and kept the melt at this temperature for 1 h till a bubble free liquid was formed. The crucibles were shaken frequently for the homogeneous mixing of all the constituents. The resultant melt was poured on a rectangular brass mould (having smooth polished inner surface) held at room temperature. The samples were subsequently annealed at 450 ºC in another furnace. The results indicate that the actual glass compositions are essentially equal to those based on the glass batch. The glasses were then ground and optically polished.

The density 'd' of these glasses was determined by the standard principle of Archimedes' using xylene (99.99 % pure) as the buoyant liquid. The glass transition temperatures of these

glasses were determined by differential scanning calorimetry traces recorded using universal V23C TA differential scanning calorimeter. The IR transmission spectra of these glasses in KBr matrices were recorded using Perkin-Elmer 283B spectrophotometer in the frequency range 4000-400 cm^{-1}. X-Ray irradiation on these glasses was carried out at room temperature for 1 h with an X-ray tube operated at 35 kV, 10 mA. The optical absorption spectra of these glasses were recorded (before and after X-ray irradiation) on Shimadzu-3101 pc UV-vis-NIR spectrophotometer in the wavelength range 250-2100 nm. The thermoluminescence glow curves of these glasses were recorded on computerized Nucleonix-thermoluminescence set up (Nucleonix Pvt. Ltd., Hyderabad, India) in the temperature range 303-573 K; the rate of heating of the glasses was maintained at 1 ºC/s.

RESULTS AND DISCUSSION

From the measured values of density and the average molecular weight M various other physical parameters such as rare earth ion concentration N_i, mean manganese ion separation distance are calculated and presented in the Table-1.

The curves obtained from differential scanning calorimetric study for the pure Li_2O-MO-B_2O_3 glasses is presented in Fig. 1. All the pure glasses exhibit an endothermic effect due to the glass transition temperature T_g between 537 and 553 ºC (Table-2). Presence of single transition temperature T_g indicates homogeneity of the glass. At higher temperatures, an exothermic peak T_c due to the crystal growth followed by an endothermic effect due to the re-melting of the glass symbolized by T_m are observed. The glass forming ability (Hruby's) parameter $K_{gl} = (T_c - T_g)/(T_m - T_c)$ is calculated, which give the information about the stability of the glass against devitrification[8,9] are evaluated and presented in Table-2.

Fig. 2 represents the thermograms of Li_2O-ZnO-B_2O_3: Ln_2O_3 glasses; for these rare earth doped glasses the glass transition temperature T_g is in between 547.6 and 550 ºC. For all glasses with the increase in the atomic number Z of the rare earth ions the values of T_g and T_c-T_g is found to increase gradually. Thermograms recorded for the CaB and CdB series of the glasses have also exhibited similar behaviour. Among the three series, the highest values of these parameters are obtained

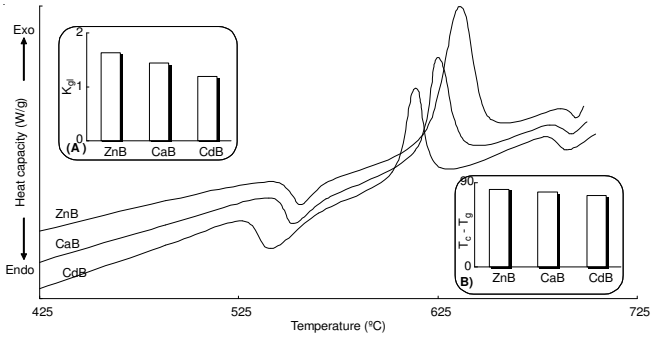

Fig. 1. DSC patterns Li_2O-MO-B_2O_3 glasses; insets (A) represents the variation of Hruby's parameter and (B) gives the vsariation of T_c - T_g values for different modifiers

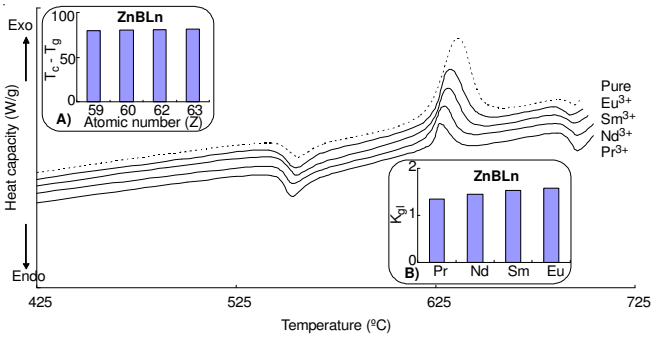

Fig. 2. Thermograms of rare earth doped Li_2O-ZnO-B_2O_3 glasses. Insets (A) gives the variation of (T_c-T_g) with the atomic No. Z of the rare earth ion (B) gives the variation of Hruby's parameter for Ln^{3+} doped Li_2O-ZnO-B_2O_3 glasses

for ZnO modifier glass doped with any rare earth ion (Fig. 2) indicating its relatively high glass forming ability; for the other two series of glasses the Hruby's parameters are decreased indicating its relatively low glass forming ability.

The infrared transmission spectra of pure Li_2O-Mo-B_2O_3 glasses (Fig. 3) exhibit two groups of bands: (i) in the region 1600-1200 cm^{-1}, (ii) in the region 1200-800 cm^{-1} and (iii) a band at about 710 cm^{-1}. It is well known that the effect of introduction of alkali oxides into B_2O_3 glass is the conversion of sp^2 planar BO_3 units into more stable sp^3 tetrahedral BO_4 units and may also create non-bridging oxygens. Each BO_4 unit is linked to two such other units and one oxygen from

TABLE-1
VARIOUS PHYSICAL PROPERTIES OF Li_2O-MO-B_2O_3:Ln^{3+} GLASSES (M = Zn, Ca or Cd)

Glass	d (g/cm^3)	$\overline{M}$	N_i (10^{22} ions/cm^3)	R_i (Å)	R_p (Å)	F_i (10^{17} cm^{-2})	n_d
ZnB	2.181	46.001	–	–	–	–	1.517
ZnBPr	3.067	44.818	4.122	2.895	1.166	2.205	1.528
ZnBNd	3.024	44.824	4.063	2.909	1.172	2.184	1.524
ZnBEu	2.916	44.831	3.918	2.944	1.186	2.131	1.523
ZnBSm	2.839	44.833	3.814	2.971	1.197	2.094	1.521
CaB	2.415	46.017	–	–	–	–	1.519
CaBPr	3.192	44.820	4.290	2.857	1.151	2.264	1.530
CaBNd	3.087	44.826	4.148	2.889	1.164	2.214	1.527
CaBEu	3.023	44.827	4.062	2.909	1.172	2.183	1.525
CaBSm	2.972	44.832	3.993	2.926	1.179	2.159	1.522
CdB	2.799	46.028	–	–	–	–	1.523
CdBPr	3.443	44.831	4.625	2.786	1.123	2.381	1.538
CdBNd	3.329	44.835	4.472	2.817	1.135	2.328	1.531
CdBEu	3.221	44.839	4.326	2.849	1.148	2.277	1.529
CdBSm	3.118	44.841	4.187	2.880	1.160	2.228	1.524

TABLE-2
DATA ON DIFFERENTIAL SCANNING CALORIMETRIC (DSC) STUDIES OF Li_2O-MO-B_2O_3: Ln_2O_3 GLASSES (M = Zn, Ca or Cd)

Glass	T_g (ºC)	T_c (ºC)	T_m (ºC)	T_g/T_m	(T_c-T_g) (ºC)	$\frac{(T_c - T_g)}{T_m}$	K_{gl}
ZnB	553.0	636.0	686.7	0.805	83.0	0.121	1.637
ZnBPr	547.6	627.0	686.0	0.798	79.4	0.116	1.346
ZnBNd	548.3	629.0	685.2	0.800	80.7	0.118	1.436
ZnBSm	549.8	631.0	684.0	0.804	81.2	0.119	1.532
ZnBEu	550.0	632.0	684.0	0.804	82.0	0.120	1.577
CaB	544.7	625.0	681.0	0.800	80.3	0.118	1.434
CaBPr	536.9	613.0	678.0	0.792	76.1	0.112	1.171
CaBNd	538.6	615.0	678.0	0.794	76.4	0.113	1.213
CaBSm	541.0	618.0	679.0	0.797	77.0	0.113	1.262
CaBEu	543.2	622.0	680.0	0.799	78.8	0.116	1.359
CdB	537.0	613.8	678.0	0.792	76.8	0.113	1.196
CdBPr	532.0	607.0	679.0	0.784	75.0	0.110	1.042
CdBNd	533.0	608.5	678.0	0.786	75.5	0.111	1.086
CdBSm	533.3	609.0	677.0	0.788	75.7	0.112	1.113
CdBEu	535.0	611.0	677.0	0.790	76.0	0.112	1.152

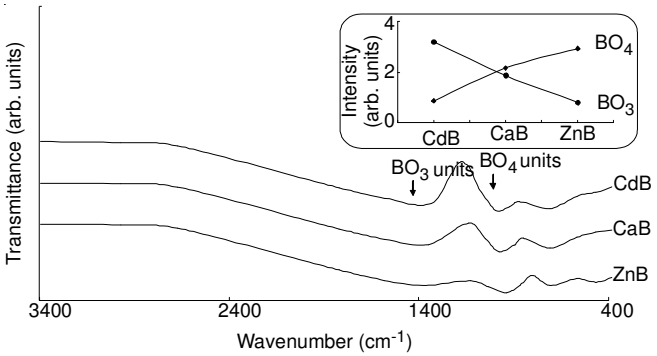

Fig. 3. Infrard spectra of Li_2O-MO-B_2O_3 glasses recorded at room temperature. Inset figure represents the variation of intensities of BO_3 and BO_4 units for different glasses

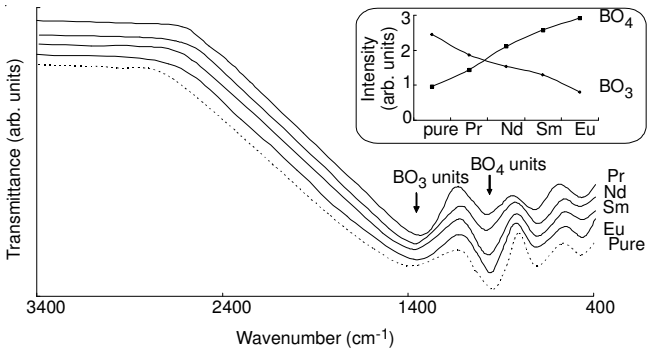

Fig. 4. Infrared spectra of Li_2O-ZnO-B_2O_3 glasses doped with Ln^{3+} ions recorded at room temperature. Inset figure represents the variation of intensities of BO_3 and BO_4 units with atomic number of rare earth ions

each unit with a rare earth ion and the structure leads to the formation of long tetrahedron chains. The second group of bands is attributed to such BO_4 units where as the first group of bands is identified as due to the stretching relaxation of the B-O bond of the trigonal BO_3 units and the band at 710 cm^{-1} is due to the bending vibrations of B-O-B linkages in the borate network[10-13]. The weak band observed around 456 cm^{-1} is an indicative of the presence of ZnO_4 units in the ZnB series glass network[14,15]. Fig. 4 represents IR spectra of the pure as well as rare earth doped Li_2O-ZnO-B_2O_3 glasses. When the glasses are doped with Ln_2O_3, the intensity of the second group of bands (band due to the trigonal BO_4 units) is found to increase at the expense of first group of bands (bands due to tetrahedral BO_3 units) with the increase of atomic number of rare earth ions with the shifting of *meta*-centres of first and second group of bands, respectively towards slightly lower and higher wave number for all the three series of glasses. (Fig. 4 represents the variation of intensities of BO_3 and BO_4 units with atomic number of rare earth ions). No significant change in position and intensity of the other bands is observed in the spectra of all the three series of the glasses by introducing the rare earth ions. The summary of the data on the positions of various bands in the IR spectra of Li_2O-MO-B_2O_3: Ln_2O_3 glasses are presented in Table-3.

TABLE-3
PEAK POSITIONS (cm^{-1}) OF IR SPECTRA OF
Li_2O-MO-B_2O_3:Ln_2O_3 GLASSES (M = Zn, Ca or Cd)

Glass	Band due to B-O bond stretching in BO_3 units (cm^{-1})	Band due to B-O bond stretching in BO_4 units (cm^{-1})	Band due to B-O-B linkage in borate network (cm^{-1})
ZnB	1378	939	710
ZnBPr	1367	954	710
ZnBNd	1360	963	710
ZnBSm	1353	975	710
ZnBEu	1337	984	710
CaB	1352	979	710
CaBPr	1343	989	710
CaBNd	1336	992	710
CaBSm	1327	1002	710
CaBEu	1319	1013	710
CdB	1336	992	710
CdBPr	1329	1008	710
CdBNd	1323	1019	710
CdBSm	1316	1027	710
CdBEu	1304	1036	710

Thermoluminescence glow curves of all the ZnB glasses doped with rare earth ions have shown in Fig. 5. Pure Li_2O-ZnO-B_2O_3 glass exhibits glow peak at 382 K. When these glasses are doped with different rare earth ions no additional

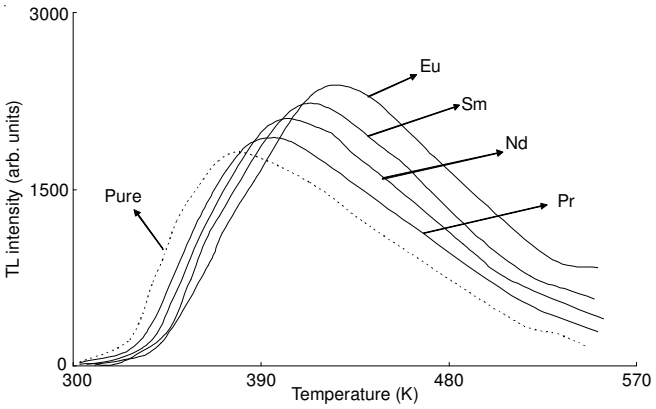

Fig. 5. Thermoluminescence out put of pure (dotted line) and Ln^{3+} doped Li_2O-ZnO-B_2O_3 glasses

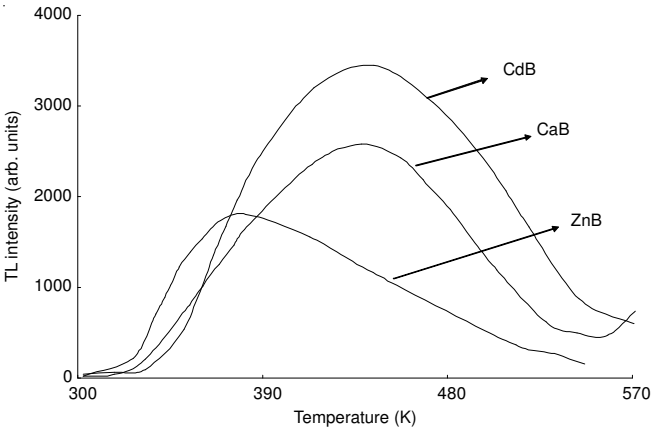

Fig. 6. Thermoluminescence of Li_2O-MO-B_2O_3 glasses

peaks are observed but the glow peak temperature T_m of the existing glow peak shifted gradually towards higher temperatures with gain in intensity of thermoluminescence light output. This trend is continued up to europium (Z = 63) doped glasses. The area under the glow curve is also found to be maximum for Eu^{3+} doped glasses. The trap depth parameters for these glow peaks are computed using Chen's formulae. The summary of the data on thermoluminescence peaks with corresponding activation energies and the trap depths of the present glasses are evaluated and furnished in Table-4.

The trap depth parameters for the glow peaks of rare earth doped CaB and CdB glasses are also computed using Chen's formulae and the summary of the data on thermoluminescence peaks with corresponding activation energies and the trap depths are evaluated and furnished in Table-4 and thermoluminescence glow curves of all the pure Li_2O-MO-B_2O_3 glasses are presented in Fig. 6.

The activation energies for these glow peaks are computed using Chen's formulae[16]:

$$E_\tau = 1.52\left(\frac{kT_m^2}{\tau}\right) - 1.58(2kT_m) \quad (1)$$

$$E_\delta = 0.976\left(\frac{kT_m^2}{\delta}\right) \quad (2)$$

for the first order kinetics.

In the above equation K is Boltzmann constant, $t = T_m - T_1$, $\delta = T_2 - T_m$, $\mu_g = \delta/(T_2 - T_1)$, where T_m = glow peak temperature, T_1 (rising end) and T_2 (falling end) are the temperatures at the half widths of the glow peaks. The summary of the data on thermoluminescence peaks with corresponding trap depth parameters of the present glasses is furnished in Table-4.

It may be noted here that prior to thermoluminescence measurements we have recorded the optical absorption spectra of all the glasses before and after X-ray irradiation. After the X-ray irradiation no additional absorption bands are observed other than those obtained in non-irradiated glasses. However the relative intensities of these bands are slightly affected. Fig. 7 presents the optical absorption spectrum of Nd^{3+} doped Li_2O-CdO-B_2O_3 glasses before and after X-ray irradiation. A similar behaviour is exhibited by all other glasses.

The action of X-ray irradiation on glasses is to produce secondary electrons from the sites where they are in a stable state and have an excess energy. Such electrons may traverse in the glass network depending upon their energy and the composition of the glass and are finally be trapped, thus forming colour centres (or alternatively they may form excitons with energy states in the forbidden gap). The trapping sites may be the rare earth ions which constitute the glass structure, ions of admixtures to the main composition and the structural defects due to impurities in the glass. Thus this process leads to the formation of (1) boron electron centres, (2) non-bridging

TABLE-4
DATA ON VARIOUS TRAP DEPTH PARAMETERS OF Li_2O-MO-B_2O_3: Ln_2O_3 GLASSES (M = Zn Ca or Cd)

Glass	T_m (K)	τ (K)	δ (K)	μ_g	E_τ (eV)	E_δ (eV)
ZnB	382	30	28	0.483	0.526	0.432
ZnBPr	386	29	27	0.482	0.560	0.458
ZnBNd	395	29	24	0.453	0.589	0.539
ZnBSm	399	28	24	0.462	0.627	0.550
ZnBEu	404	27	22	0.449	0.673	0.615
CaB	424	53	35	0.398	0.324	0.426
CaBPr	432	54	34	0.386	0.330	0.455
CaBNd	438	53	32	0.376	0.350	0.497
CaBSm	442	52	31	0.373	0.367	0.523
CaBEu	445	51	30	0.370	0.382	0.548
CdB	466	76	44	0.367	0.244	0.409
CdBPr	469	74	43	0.368	0.258	0.424
CdBNd	475	72	40	0.357	0.277	0.468
CdBSm	482	72	38	0.345	0.287	0.507
CdBEu	486	68	37	0.352	0.318	0.530

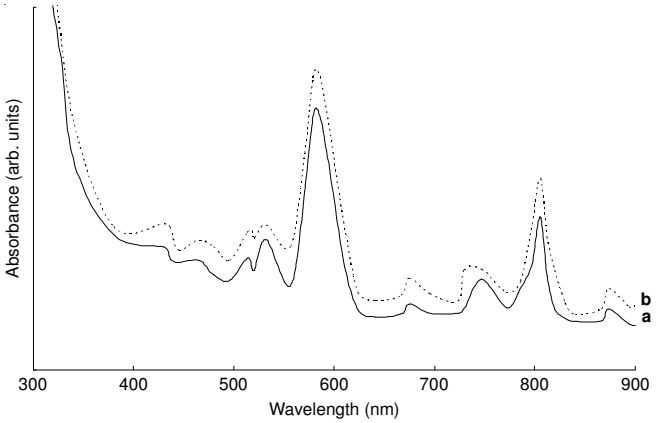

Fig. 7. Optical absorption spectrum Li_2O-CdO-B_2O_3 glasses doped with Nd^{3+} ions. (a) before and (b) after X-ray irradiation

oxygen hole centres and (3) boron oxygen hole centres. Thermoluminescence is a consequence of radiative recombination between the electrons (released by heating from electron centre) and an antibonding molecular orbital of the nearest of the oxygen hole centres.

The observed thermoluminescence peaks in the present glasses can be attributed due to such radiation. From optical absorption spectral profiles Judd-Ofelt parameters are calculated. Out of the three Judd-Ofelt parameters, Ω_4 and Ω_6 values depend strongly on the vibrational frequencies of Ln^{3+} ions linked to the ligand atoms. The values of these parameters obtained for these glasses are found to be lower for Eu^{3+} ions (Fig. 8). This indicates that the vibrational transitions are less intense for Eu^{3+} ions of the series, which may be more

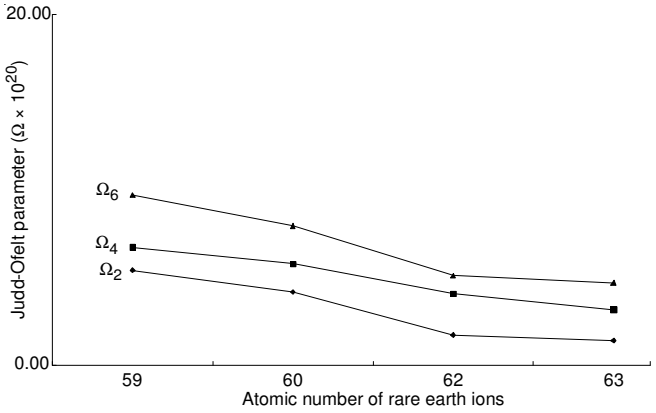

Fig. 8. Variation of Judd-Ofelt parameters for CaBLn glasses with the atomic number of rare earth ions

favourable for the formation of high concentration of colour centers at deeper depths in these glasses; the maximum thermoluminescence output at higher temperatures obtained for the Eu^{3+} ions doped glasses can be attributed due to these reasons.

It is well known that the effect of introduction of alkali oxides into B_2O_3 is the conversion of sp^2 planar BO_3 units into more stable sp^3 tetrahedral BO_4 units and may also create non-bridging oxygens. Each BO_4 unit is linked to two such other units and one oxygen from each unit with a metal ion and the structure leads to the formation of long chain tetrahedron. The presence of such BO_4 units in the present glasses is evident from the IR spectral studies.

Conclusion

Finally present studies on thermoluminescence of different rare-earth ions doped Li_2O-MO-B_2O_3 glasses indicates that Eu^{3+} ions doped glasses can be used more effectively in radiation dosimetry since they exhibit high thermoluminescence light output in high temperature region.

REFERENCES

1. W.M. Pontuschka, S. Isotani and A. Piccini, *J. Am. Ceram. Soc*., **70**, 59 (1987).
2. S.M. Del Nery, W.M. Pontuschka, S. Isotani and C.G. Rouse, *Phys. Rev*., **49B**, 3760 (1994).
3. H.B. Pascoal, W.M. Pontuschka and H. Rechenberg, *J. Non-Crystall. Solids*, **258**, 92 (1999).
4. W.M. Pontuschka, L.S. Kanashiro and L.C. Courrol, *Glass Phys. Chem*., **27**, 37 (2001).
5. A. Paul, Chemistry of Glasses, Chapman & Hall, London (1982).
6. S.R. Elliot, Physics of Amorphous Materials, Longman, London (1990).
7. J.F. Shackl Ford, Introduction to Materials Science for Engineers, Macmillan, New York (1985).
8. A. Dietzel, *Glasstech. Ber*., **22**, 41 (1968).
9. H. Ruby, *Czech. J. Phys*., **32B**, 1187 (1972).
10. R.P. Tandon and S. Hotchandani, *Phys. Stat. Sol.*, **185(a)**, 453 (2001).
11. H.H. Qiu, H. Sakata and T. Hirayama, *J. Ceram. Soc. (Japan)*, **103**, 32 (1995).
12. F.A. Khalifa and A. Azooz, *Ind. J. Pure. Appl. Phys.*, **36**, 314 (1998).
13. A.A. Ahmed and M.R. Eltohamy, *Ind. J. Pure. Appl. Phys*., **36**, 335 (1998).
14. P. Subbalakshmi and N. Veeraiah, *Ind. J. Eng. Mater. Sci*., **8**, 275. (2001).
15. B. Karthikeyan, S. Mohan and M.L. Baesso, *Physica*, **337B**, 249 (2003).
16. R. Chen, *J. Appl. Phys*., **40**, 570 (1969).